



저작자표시-비영리-변경금지 2.0 대한민국

이용자는 아래의 조건을 따르는 경우에 한하여 자유롭게

- 이 저작물을 복제, 배포, 전송, 전시, 공연 및 방송할 수 있습니다.

다음과 같은 조건을 따라야 합니다:



저작자표시. 귀하는 원저작자를 표시하여야 합니다.



비영리. 귀하는 이 저작물을 영리 목적으로 이용할 수 없습니다.



변경금지. 귀하는 이 저작물을 개작, 변형 또는 가공할 수 없습니다.

- 귀하는, 이 저작물의 재이용이나 배포의 경우, 이 저작물에 적용된 이용허락조건을 명확하게 나타내어야 합니다.
- 저작권자로부터 별도의 허가를 받으면 이러한 조건들은 적용되지 않습니다.

저작권법에 따른 이용자의 권리는 위의 내용에 의하여 영향을 받지 않습니다.

이것은 [이용허락규약\(Legal Code\)](#)을 이해하기 쉽게 요약한 것입니다.

[Disclaimer](#)

공학석사학위논문

양면 국부화 아노다이징을 이용한  
절연성 산화 알루미늄 패턴 가공

**Fabrication of insulative aluminum oxide  
patterns using two-face local anodization**

2016 년 7 월

서울대학교 대학원

기계항공공학부

정 규 강

## Abstract.

In this study, a two-face local anodization process was developed. Two-face local anodization has advantages over existing local anodization in increasing productivity and aspect ratio. Using this process, insulative aluminum oxide patterns that penetrated the base material were fabricated on 40- $\mu\text{m}$ -thick aluminum foil by approaching two identical electrodes toward both sides. The electrodes were shaped with the desired design patterns via embossing. This study consists of three parts. First, the two-face local anodization system was developed. Second, a parameter study was undertaken to determine the optimum experimental conditions, as the proper applied voltage, gap between electrode and workpiece, and pulse condition were required for localization and reaction efficiency. Third, a single layer RF antenna was manufactured to verify the effectiveness of the process, and its performance was proven by PSA spectrum analyzer.

**Keywords:** local anodization, local anodic oxidation, aluminum oxide, micro electrochemical machining

**Student Number:** 2014-22503

# Table of Contents

Abstract .....	i
Contents .....	ii
List of Figures .....	iii
List of Tables .....	v
Chapter 1. Introduction .....	1
Chapter 2. Two-face local anodization process development .....	6
Chapter 3. Parameter study .....	12
Chapter 4. Experimental results and analysis .....	20
Chapter 5. Application .....	23
Chapter 6. Conclusion .....	26
Reference .....	27
국문 초록 .....	30

## List of Figures

- Figure 1. Schematic diagram of conventional aluminum anodization process.
- Figure 2. Principle of aluminum oxide thickness growth
- Figure 3. Double layer model
- Figure 4. Difference of charging potential between small  $R_s$  and large  $R_s$
- Figure 5. Schematic diagram of experimental setup.
- Figure 6. (a) Position of tool electrodes and workpiece(aluminum foil), (b) surface image of fabricated aluminum oxide insulation, (c) cross section view of aluminum oxide growth according to time (0, 10, 25 min)
- Figure 7. Schematic diagram and 3D image of experimental results for each experimental steps. (a), (d): without flushing and without coating, (b), (e): with flushing and without coating, (c), (f): with flushing and with coating.
- Figure 8. Surface image of fabricated aluminum oxide in different inter-electrode gap condition (a) 20  $\mu\text{m}$ , (b) 30  $\mu\text{m}$ , (c) 40  $\mu\text{m}$ , (d) 50  $\mu\text{m}$ , (e) 60  $\mu\text{m}$ .
- Figure 9. Aluminum oxide line width change according to inter-electrode gap increases.
- Figure 10. Charging voltage change according to distance from midpoint for 40 and 60  $\mu\text{m}$  inter-electrode gap.
- Figure 11. Surface image of fabricated aluminum oxide in different applied voltage condition (a) 10 V, (b) 15 V, (c) 20 V, (d) 25 V, (e) 30 V.
- Figure 12. Aluminum oxide line width change according to applied voltage increases

- Figure 13. Charging voltage change according to distance from midpoint for 10, 15, 20, 25 and 30 volts applied.
- Figure 14. Aluminum oxide line width and anodization time for insulation change according to pulse frequency changes.
- Figure 15. Cross section view of aluminum oxide growth according to anodization time in one-face local anodization process. (a) 6 min, (b) 9 min, (c) 12 min, (d) 15 min, (e) 18 min.
- Figure 16. Surface image and cross section view of one-face and two-face local anodization process.
- Figure 17. Comparison between one-face and two-face local anodization process in fabricated aluminum oxide line width and anodization time for insulation.
- Figure 18. (a) RF antenna design and (b) schematic diagram of experiment.
- Figure 19. (a) Fabricated RF antenna and (b) its absorbing performance as measured by spectrum analyzer.

## List of Tables

Table 1. Experimental condition for process improvement

Table 2. Experimental condition for gap between tool and workpiece parameter study

Table 3. Experimental condition for applied voltage parameter study

Table 4. Experimental condition for RF antenna fabrication

# Chapter 1.

## Introduction

### 1.1. Study background

Aluminum oxide ( $\text{Al}_2\text{O}_3$ ) is a reliable insulating material with good wear resistance and high thermal conductivity. Its electrical resistance is approximately  $1.00\text{e}+14\text{ohm-cm}$ . For its outstanding mechanical and chemical properties, it is widely used in various applications such as surface protection, heat sinks, and electronic substrate; however, most applications involve the overall surface oxidation of bulk aluminum.

There have been several previous studies on fabricating aluminum oxide patterns locally. The idea of local anodization is derived from scanning probe microscopes (SPM) or atomic force microscope (AFM) [1, 2]. The studied techniques are limited in that they can only anodize to a thickness of several tens of nanometers. The limitation of the thickness of AAO expanded by applying Mott-Cabrera model [3] and double layer model [4]. Jee et al [5] fabricated insulative aluminum oxide on aluminum foil in micro scale. However, this technique has problems of low productivity and low aspect ratio because its method is based on tool transfer of oxide. In this study, two-face local anodization was proposed. The concept of this process is from die-sinking



electro discharge machining[6] and two-face etching[7-9]. Aluminum oxide was fabricated as designed patterns without tool transfer. In addition, aluminum oxide is grown on both side of the aluminum foil. Accordingly, high productivity and aspect ratio can be achieved.

## 1.2. Background theory

### 1.2.1. Aluminum anodization

Aluminum anodizing process, which is a kind of after treatment process, fabricate oxide layer over metal surface. Increasing oxide layer thickness has advantage in strengthening corrosion and wear resistance. Moreover, oxide layer is more adhesive to paint so that anodizing process is conducted prior to coloring.

Aluminum anodization process is briefly illustrated in figure 1. Aluminum and counter electrode is sinked in acid electrolyte. Sulfuric acid is the most widely used for electrolyte and Stainless steel or tungsten carbide is used for counter electrode. After sinking, voltage is applied to aluminum and counter electrode; plus voltage to aluminum and minus voltage to counter electrode.

Aluminum oxide layer thickness grows as a result of two chemical reaction; formation of oxide layer and dissolution of aluminum oxide. These two chemical reactions occurs simultaneously and consequently fabricate porous aluminum oxide layer. The schematic diagram of aluminum anodization is shown in figure 2.

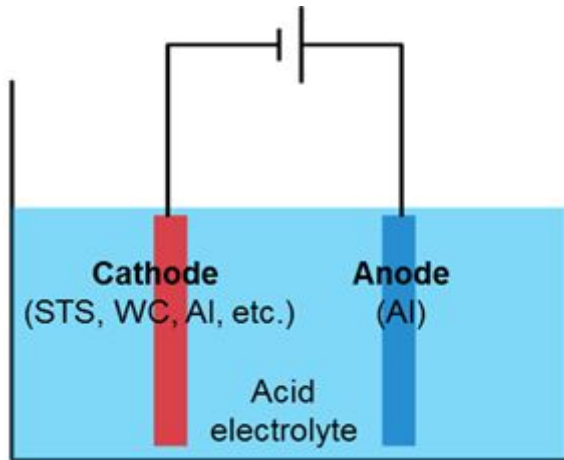


Figure 1. Schematic diagram of conventional aluminum anodization process.

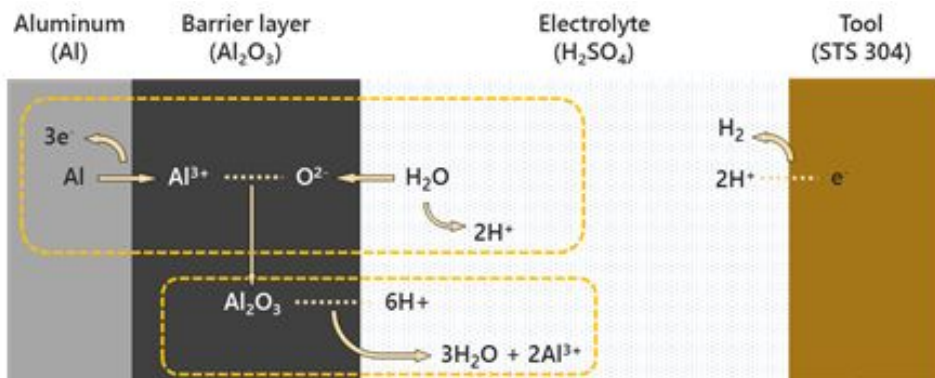


Figure 2. Principle of aluminum oxide thickness growth[23].

## 1.2.2. Principle of local anodization

The principle of local anodization is based on micro electro chemical machining. In micro ECM, localization is explained with double layer theory (Figure 3). The electrode and workpiece is placed close to each other then pulsed voltage is applied. In double layer theory, the electrolyte between electrode and workpiece is illustrated as an equivalent RC circuit. The electrolyte resistance ( $R_s$ ) increases as distance between electrode and workpiece increases.

In RC circuit system, voltage increase exponentially when capacitor voltage is applied (1.1). The voltage increases faster with smaller electrolyte resistance (figure 4). In formula 1.2 R, which is electrolyte resistance, equals to  $\rho$  (specific electrolyte resistance) times  $d$  (distance between electrode and workpiece). Therefore the electrolyte resistance is small near the tool electrode since the smaller distance.

$$V(t) = V_0 e^{-\frac{t}{RC}} \quad (1.1)$$

$$R = \rho \times d \quad (1.2)$$

When applied pulsed voltage with short pulse on time, potential can be increase over effective potential for reaction near the electrode. As a result, aluminum oxide can be formed near the electrode.

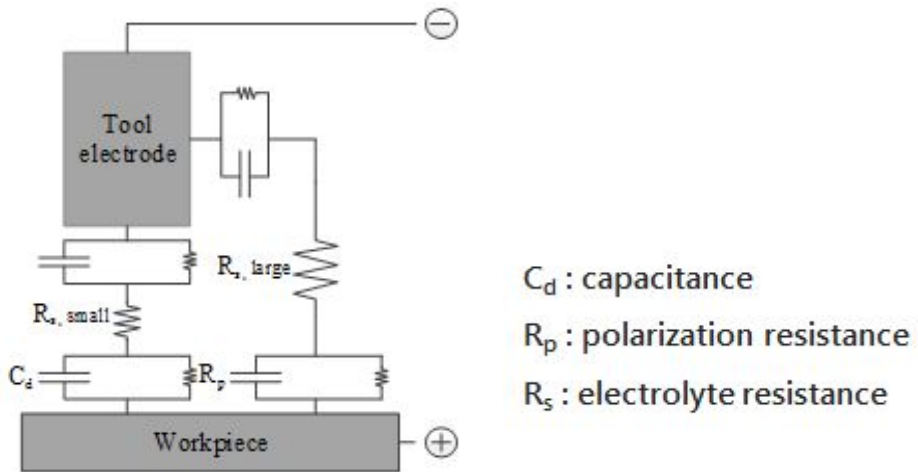


Figure 3. Double layer model [24]

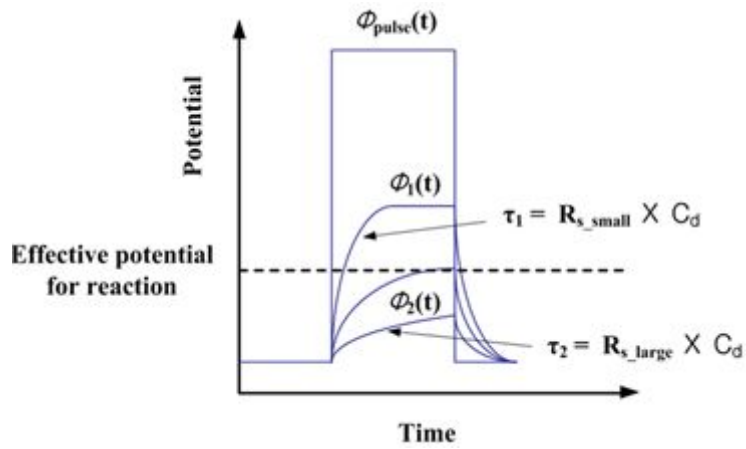


Figure 4. Difference of charging potential between small  $R_s$  and large  $R_s$  [24]

## Chapter 2

### Two-face local anodization process development

#### 2.1. Experimental condition

Highly pure 40- $\mu\text{m}$ -thick aluminum foil (99.999%, Nilaco Co.) was used as a workpiece. Aluminum foil is cleaned with  $\text{C}_2\text{H}_5\text{OH}$  solution and DI water before anodizing. Stainless steel 304 is used as the tool electrode. The tool surface, where the chemical reactions take place, is smoothen with 1500 grit sandpaper. After then it also cleaned with  $\text{C}_2\text{H}_5\text{OH}$  solution and DI water.

The aluminum foil was anodized in mixture of 0.5 M sulfuric acid ( $\text{H}_2\text{SO}_4$ ) and 0.5 M oxalic acid ( $\text{C}_2\text{H}_2\text{O}_4$ ) solution (50:50 volume ratio) at room temperature. The concentration of electrolyte is chosen for avoiding anodizing defects [10, 11] and the mixture ratio is based on previous research [5].

Pulsed voltage is used in the anodizing process. Pulse voltage is practical to fabricate aluminum oxide faster and thicker than constant voltage [12]. An 8551 pulse generator (Tabor Electronics) and power supply are used to control the pulse-on-time, pulse duration, and amplitude of the applying pulses.

The electrode position is controlled with a motor driven stage system. The X–Y stage is controlled by a 315082AT (Parker Automation) and the Z stage by a 4042200XR (Parker Automation). The gap between workpiece and electrode is controlled by manual input with 2.5  $\mu\text{m}$  resonance.

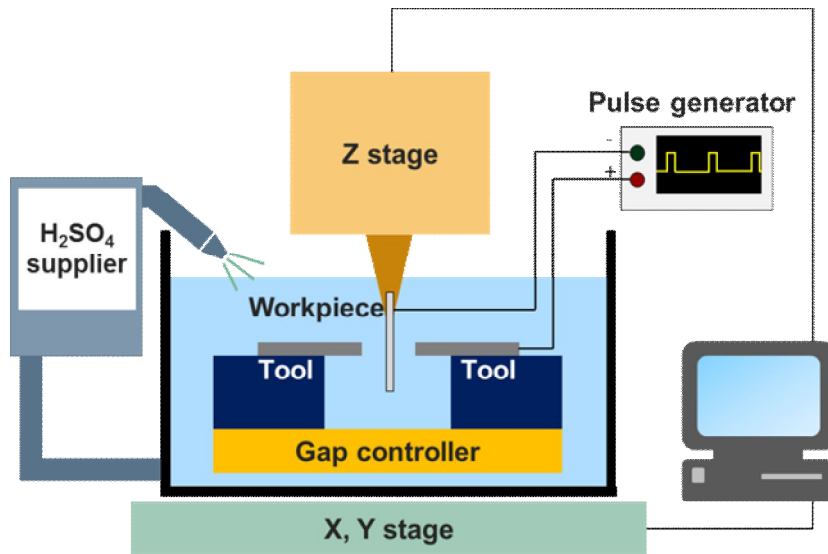


Figure 5. Schematic diagram of experimental setup.

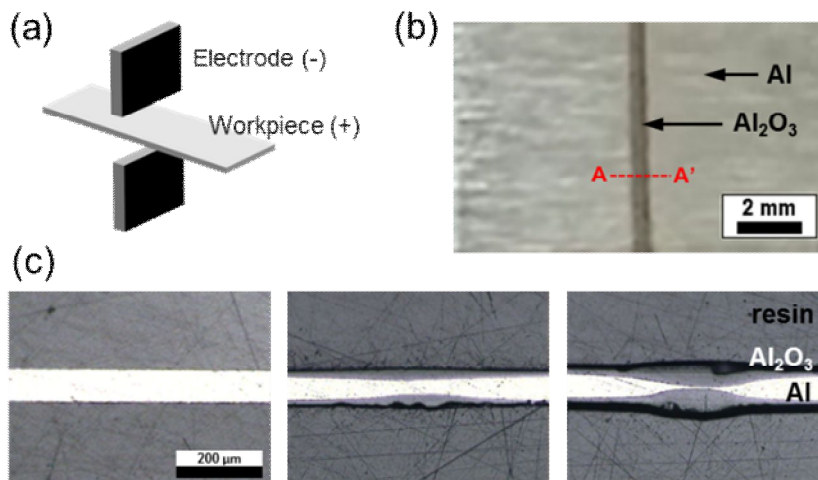


Figure 6. (a) Position of tool electrodes and workpiece(aluminum foil), (b)surface image of fabricated aluminum oxide insulation, (c)cross section view of aluminum oxide growth according to time (0, 10, 25 min)

## **2.2. Process improvement**

### **2.2.1. Flushing**

Experiment for process improvement was conducted. The experimental condition is stated in table 1. During the anodization process, hydrogen gas is created on the tool electrodes. Hydrogen bubbles, which are generated on both top and bottom surfaces of tool electrodes, act as coating so that the aluminum oxide boundary line was definite. Hydrogen bubbles generated between the tool electrodes and aluminum foil disturb the anodization process. Therefore, flushing out these bubbles is required. A pump system pours electrolyte on the area where anodization occurs; thus, a continuous chemical reaction is possible. (Figure 5)

As a result of the flushing system, the aluminum oxide was formed evenly; however, the boundary line of the aluminum oxide was blurred. (Figure 7) Since the hydrogen bubbles on top and bottom surface acted as coating material, flushing out the bubbles makes the sides of tool electrode participate in the chemical reaction.

### **2.2.2. Electrode coating**

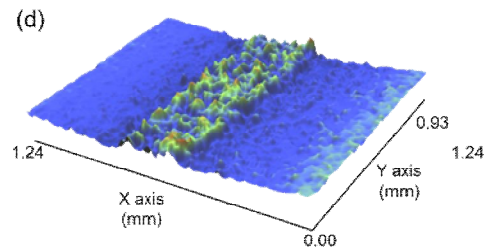
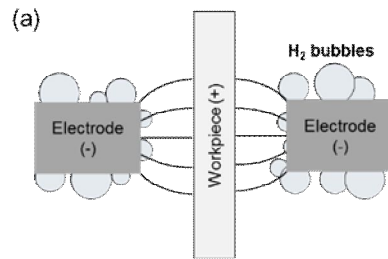
The aluminum oxide boundary was blurred after the flushing system was installed. To localize the anodization area, the top and bottom surfaces of tool electrodes were coated with enamel for its non-conductivity and adhesiveness. Enamel coated the whole surface of the tool electrodes except for the reaction area. As a result, a definite aluminum oxide boundary line was achieved. The aluminum oxide was also fabricated evenly and sufficiently. (Figure 3)



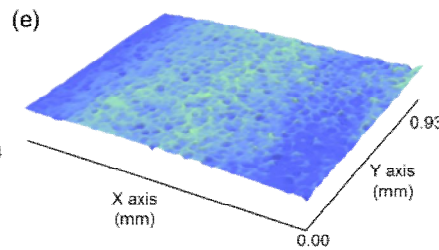
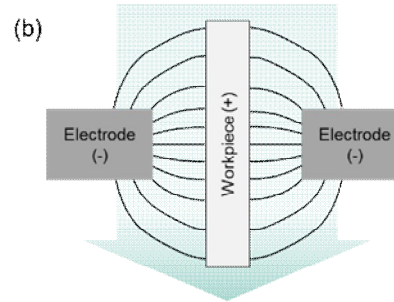
Item	Specification
Tool	304 STS (200 $\mu\text{m}$ )
Workpiece	Al foil (40 $\mu\text{m}$ ) (5 mm $\times$ 20 mm)
Inter-electrode gap	50 $\mu\text{m}$
Applied voltage	20 V
Pulse on time	1 $\mu\text{s}$
Pulse period	5 $\mu\text{s}$
Electrolyte	H <sub>2</sub> SO <sub>4</sub> 0.5 M + C <sub>2</sub> H <sub>2</sub> O <sub>4</sub> 0.5 M

Table 1. Experimental condition for process improvement

**Without flushing & without coating**



**Flushing & without coating**



**Flushing & Coating**

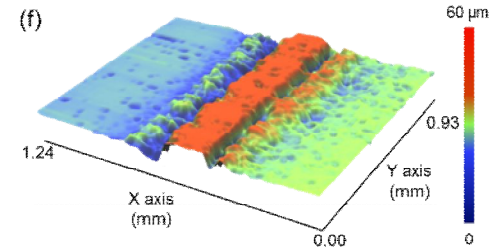
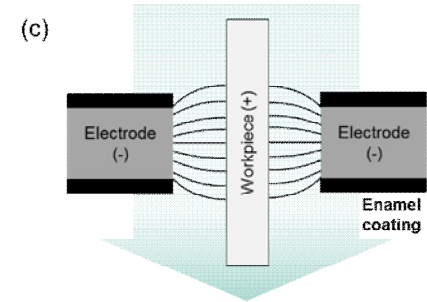


Figure 7. Schematic diagram and 3D image of experimental results for each experimental steps. (a), (d): without flushing and without coating, (b), (e): with flushing and without coating, (c), (f): with flushing and with coating.

## Chapter 3.

### Parameter study

#### 3.1. Gap between tool electrode and workpiece

A parameter study was conducted to determine the effects of various factors on the process. According to previous researches, the gap between tool electrode and workpiece is the main factor that affects aluminum oxide line width. Therefore, the parameter study was conducted with the inter-electrode gap changed from 20 to 60  $\mu\text{m}$  at 10  $\mu\text{m}$  intervals. The experimental condition is stated in table 2. The experimental results are shown in figure 8.

The width of the aluminum oxide line increases as the inter-electrode gap increases. With a 30- $\mu\text{m}$  inter-electrode gap configuration, the boundary line was indefinite and aluminum oxide was insufficiently thick. The inter-electrode gap was so narrow that the hydrogen bubbles could not be flushed properly. Over a 50- $\mu\text{m}$  gap configuration, the boundary line was blurred. The charging voltage decreases according to distance from the midpoint because of high electrolyte resistance[13]. The maximum charging voltage is lower and the charging voltage declines more slowly in a wide inter-electrode configuration (Figure 10). The chemical reaction rate is exponential to charging voltage therefore, at 60  $\mu\text{m}$ , an insufficiently thick oxide layer and blurred boundary line were produced.

Item	Specification
Electrode	304 STS (200 $\mu\text{m}$ )
Workpiece	Al foil (40 $\mu\text{m}$ ) (5 mm $\times$ 20 mm)
Inter-electrode gap	40 $\mu\text{m}$
Pulse on time	2 $\mu\text{s}$
Pulse period	10 $\mu\text{s}$
Anodization time	5 min
Electrolyte	$\text{H}_2\text{SO}_4$ 0.5 M + $\text{C}_2\text{H}_2\text{O}_4$ 0.5 M

Table 2. Experimental condition for gap between tool and workpiece parameter study

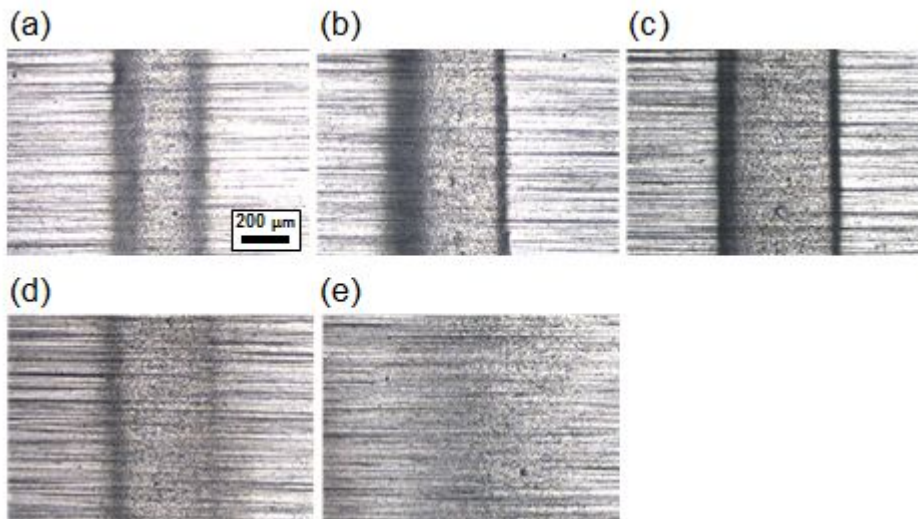


Figure 8. Surface image of fabricated aluminum oxide in different inter-electrode gap condition (a) 20  $\mu\text{m}$ , (b) 30  $\mu\text{m}$ , (c) 40  $\mu\text{m}$ , (d) 50  $\mu\text{m}$ , (e) 60  $\mu\text{m}$ .

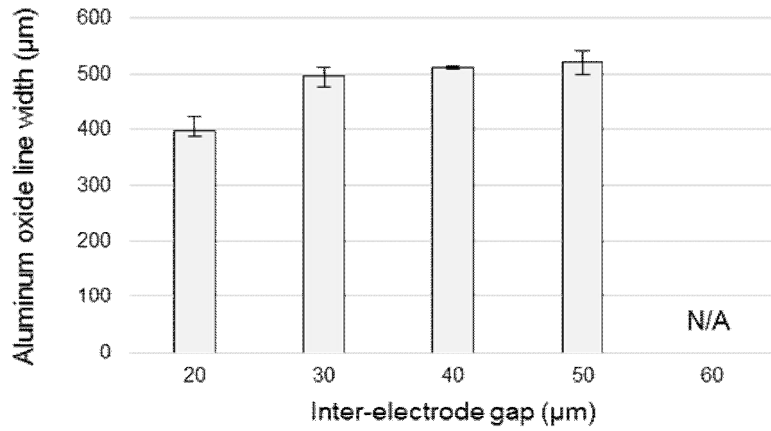


Figure 9. Aluminum oxide line width change according to inter-electrode gap increases.

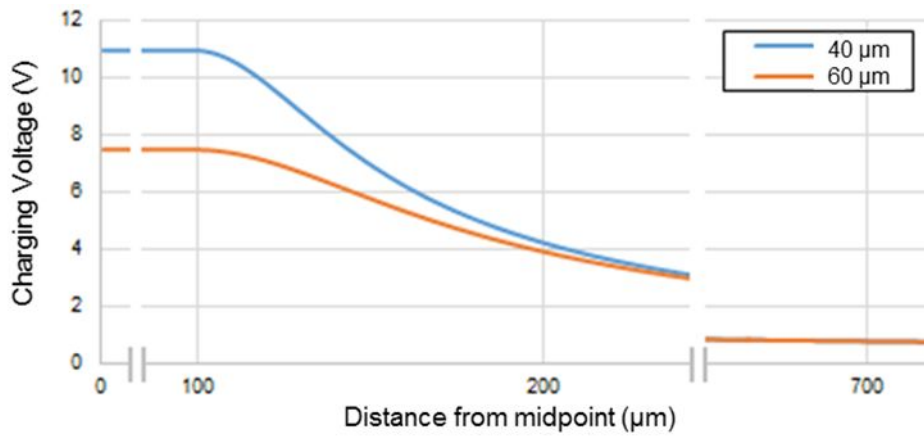


Figure 10. Charging voltage change according to distance from midpoint for 40 and 60  $\mu\text{m}$  inter-electrode gap.

## 3.2. Applied voltage

Applied voltage affects localization as inter-electrode gap does[14]. Applied voltage is also directly proportional to current density, which has an effect on thickness and morphology of AAO[15]. The parameter study was conducted by varying the applied voltage from 10 V to 30 V at 5 V intervals. The experimental condition is stated in table 3. The experimental results are shown in figure 11.

The line width and thickness of aluminum oxide increased as applied voltage increases. The aluminum oxide line was indefinite and the aluminum oxide thickness was under 10  $\mu\text{m}$  at 10 and 15 V. Over 25 V, the thickness of the aluminum oxide layer was over 30  $\mu\text{m}$  but the aluminum oxide line spread beyond the area desired to be anodized. This phenomena can also be explained with double layer theory. The current density increases as charging voltage increases. Because of low current density, a thin aluminum oxide layer was obtained at low voltages. In high applied voltage condition, the boundary line spread since current sufficient to anodize can flow in a wider area.

Item	Specification
Tool	304 STS (200 $\mu\text{m}$ )
Workpiece	Al foil (40 $\mu\text{m}$ ) (5 mm $\times$ 20 mm)
Inter-electrode gap	40 $\mu\text{m}$
Applied voltage	20 V
Electrolyte	$\text{H}_2\text{SO}_4$ 0.5 M + $\text{C}_2\text{H}_2\text{O}_4$ 0.5 M

Table 3. Experimental condition for applied voltage parameter study

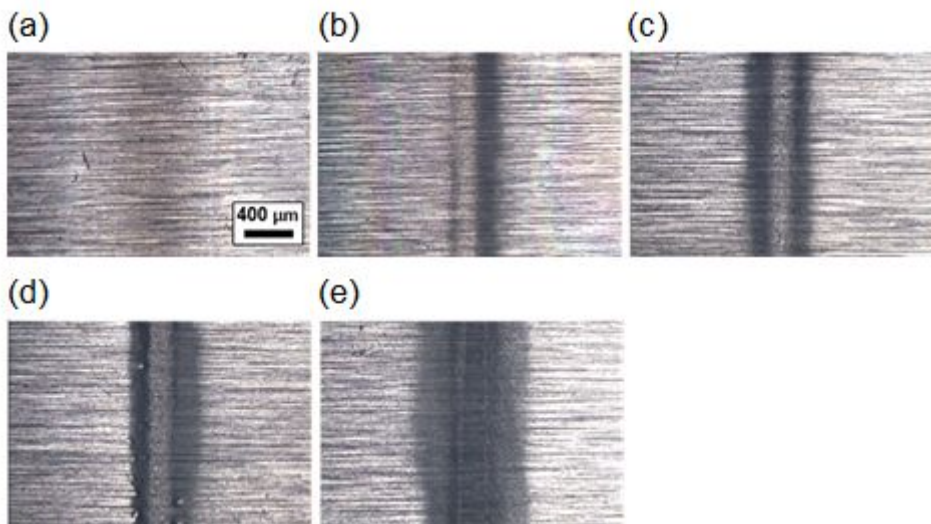


Figure 11. Surface image of fabricated aluminum oxide in different applied voltage condition (a) 10 V, (b) 15 V, (c) 20 V, (d) 25 V, (e) 30 V.

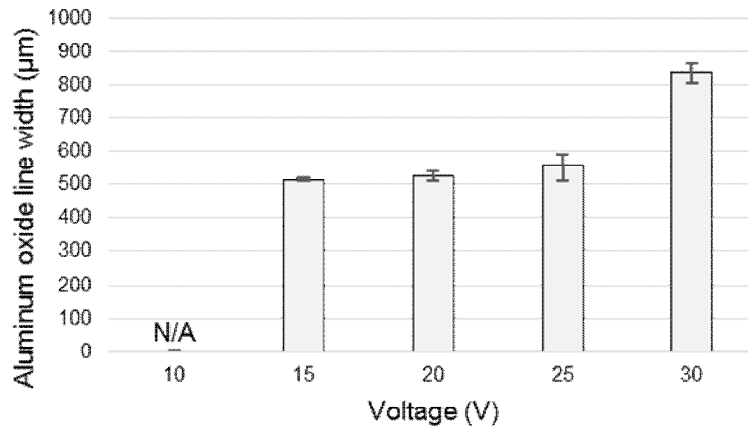


Figure 12. Aluminum oxide line width change according to applied voltage increases

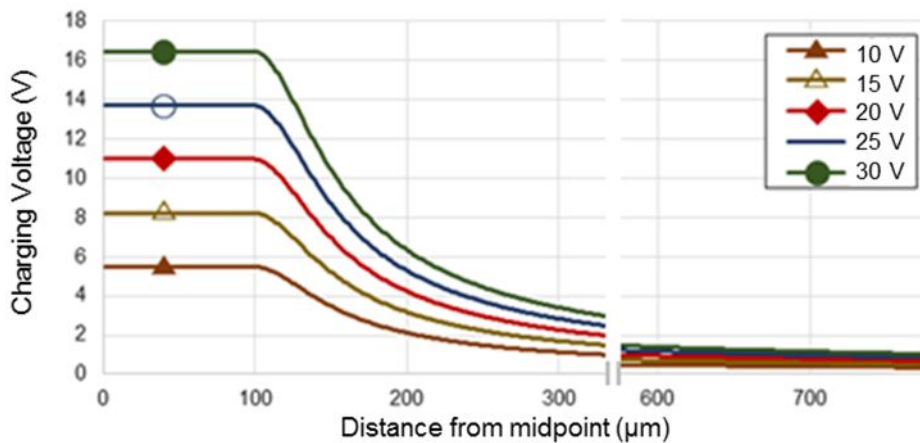


Figure 13. Charging voltage change according to distance from midpoint for 10, 15, 20, 25 and 30 volts applied.



### 3.3. Pulse condition

In the aluminum anodizing process, pulse condition influences the aspect of fabricated aluminum oxide[16]. Penetration of the aluminum oxide pattern is required for achieving insulation. Fast aluminum oxide growth in the axial direction is demanded for fabricating insulating aluminum oxide patterns.

The pulse-on-time changes from 1 to 10  $\mu$ s with a fixed duty ratio (pulse-on-time:pulse-off-time=1:5). The anodization process was maintained until the insulative barrier was obtained on 40- $\mu$ m-thick aluminum foil. The results of experiment are shown in figure 14.

The aluminum oxide line width decreased as pulse-on-time increased. This phenomena can be explained as accuracy improvement with increase of pulse-on-time[17].

In 1  $\mu$ s pulse-on-time condition, an insulative oxide barrier failed to develop over a 30 minprocess time because of low current density. When applied 10  $\mu$ s pulse-on-time, anodizing defects occurred and aluminum foil lost its original shape. Aluminum oxide grows in thickness as a result of two chemical reactions: aluminum oxidation and aluminum oxide dissolution. Anodizing defects occur when the balance between the two reactions collapses. Sulfuric acid is known to cause dissolution of aluminum oxide, and its dissolution rate increases as electrolyte temperature rises[18]. Prolonged pulse-on-time might lead to electrolyte temperature increase[19].

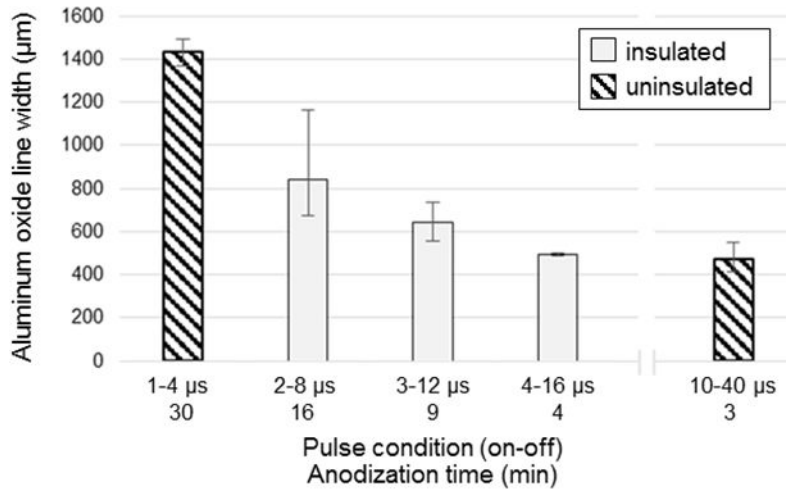


Figure 14. Aluminum oxide line width and anodization time for insulation change according to pulse frequency changes.

## Chapter 4.

### Experimental results and analysis

The objective of two-face local anodization is to attain a higher aspect ratio by improving the aluminum oxide profile, and to attain a higher overall productivity. A one-face local anodization experiment was conducted for comparison of aspect ratio and productivity. The experimental condition was decided based on a parameter study. One-face local anodization experimental results are shown in figure 15. In two-face local anodization, insulative aluminum oxide was obtained within 6 min of anodization time when using the 40- $\mu\text{m}$ -thick aluminum foil. In one-face local anodization, however, it required a longer time for obtaining insulation.

Both the thickness and line width of aluminum oxide increases as the anodization time increases. Insulative aluminum oxide was obtained in the one-face trial when anodized over 18 min, producing a line width of approximately 800  $\mu\text{m}$ . In comparison to two-face local anodization, this represents an increase in line width of approximately 25% and an increase of 175% in anodization time. In summary, improvement in aspect ratio and productivity was acquired with the two-face local anodization process.

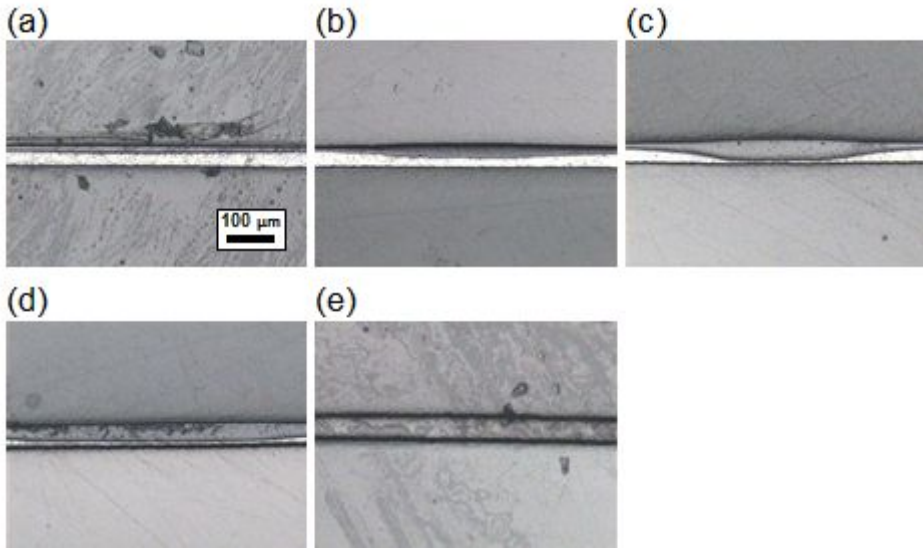


Figure 15. Cross section view of aluminum oxide growth according to anodization time in one-face local anodization process. (a) 6 min, (b) 9 min, (c) 12 min, (d) 15 min, (e) 18 min.

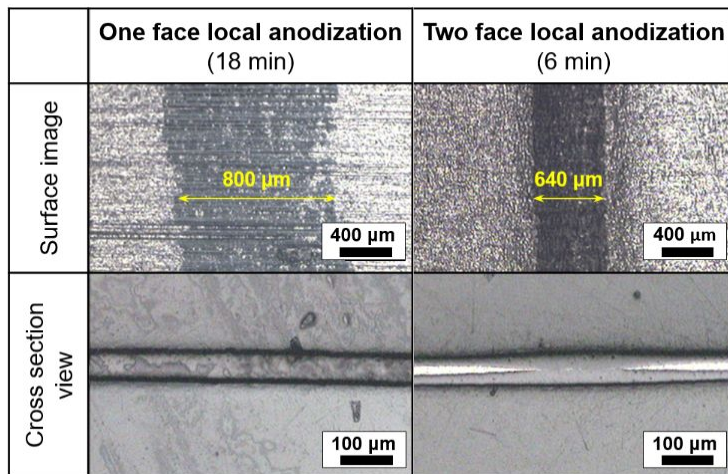


Figure 16. Surface image and cross section view of one-face and two-face local anodization process.

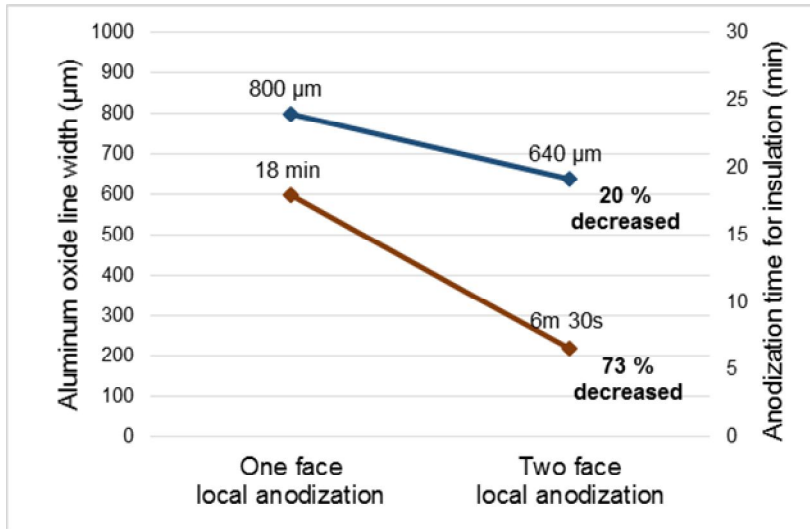


Figure 17. Comparison between one-face and two-face local anodization process in fabricated aluminum oxide line width and anodization time for insulation.

## Chapter 5.

### Application

To verify the applicability of the two-face local anodization process to a large area, a single layer RF antenna was fabricated. The experimental condition is shown in table 4. The antenna design and schematic diagram of the experiment are illustrated in figure 18 [20]. Tool electrodes are engraved in the shape of the antenna design and made of stainless steel 316l for acid-resistance.

The top view of single-layer RF antenna is shown in figure 19. The black area represents fabricated aluminum oxide. The functionality of the RF antenna is proven with spectrum analyzer E4440A PSA (Agilent Technologies). Its absorbing performance was approximately 1.93 kHz with -14.0 dB. This result shows the applicability of the two-face local anodization process to fabricate various types of single-layer electric devices[21, 22].

Item	Specification
Electrode	316l STS (200 $\mu\text{m}$ )
Workpiece	Al foil (40 $\mu\text{m}$ )
Inter-electrode gap	40 $\mu\text{m}$
Pulse on time	3 $\mu\text{s}$
Pulse period	15 $\mu\text{s}$
Anodization time	5 min
Electrolyte	$\text{H}_2\text{SO}_4$ 0.5 M + $\text{C}_2\text{H}_2\text{O}_4$ 0.5 M

Table 4. Experimental condition for RF antenna fabrication

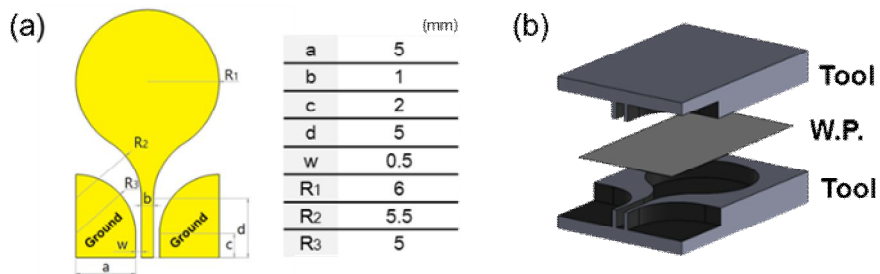


Figure 18. (a) RF antenna design and (b) schematic diagram of experiment.

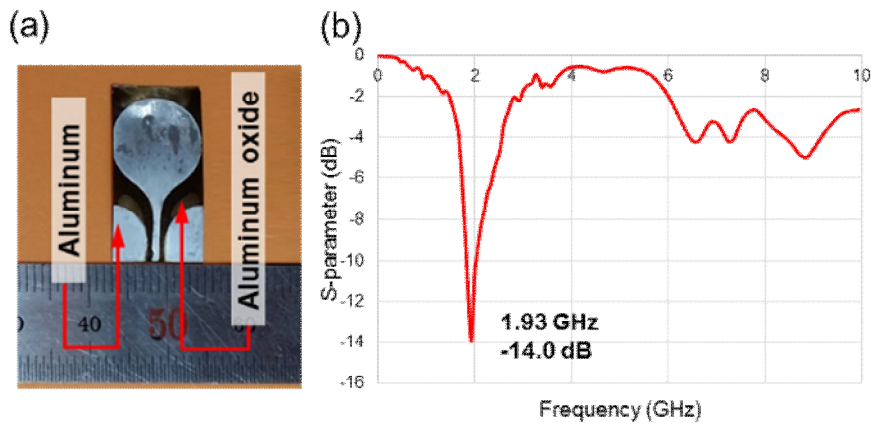


Figure 19. (a) Fabricated RF antenna and (b) its absorbing performance as measured by spectrum analyzer.



## Chapter 6.

### Conclusion

The two-face local anodization process was developed for fabricating insulative aluminum oxide patterns on aluminum foil. Flushing was helpful in maintaining a continuous chemical reaction by eliminating hydrogen bubbles, which were generated on tool electrodes. For better reaction selectivity and current density concentration, the surrounding non-reaction area of tool electrodes was coated with non-conductive material.

A parameter study was conducted to improve anodizing quality; It was designed to determine inter-electrode gap, applied voltage for localization, and pulse frequency for reaction efficiency. As a result, the optimum experimental condition was determined to be a 40  $\mu\text{m}$  inter-electrode gap, 20 V applied voltage and 3  $\mu\text{s}$  pulse-on-time. The anodization time to desired thickness was 6 min.

Two-face local anodization has advantages over one-face anodization in improving aspect ratios and productivity. In comparison with anodizing on one face, the aluminum oxide line width and anodization time were decreased by 20 % and 67 % each.

A single layer RF antenna was fabricated with 40- $\mu\text{m}$ -thick aluminum foil by the two-face local anodization process. This indicates that two-face local anodization can be applied to various types of single layer electric devices.

## Reference

1. Dagata, J., et al., Understanding scanned probe oxidation of silicon. *Applied Physics Letters*, 1998. 73(2): p. 271–273.
2. Gordon, A., et al., Mechanisms of surface anodization produced by scanning probe microscopes. *Journal of Vacuum Science & Technology B*, 1995. 13(6): p. 2805–2808.
3. Cabrera, N. and N. Mott, Theory of the oxidation of metals. *Reports on progress in physics*, 1949. 12(1): p. 163.
4. Helmholtz, H.v., Ueber einige Gesetze der Vertheilung elektrischer Ströme in körperlichen Leitern mit Anwendung auf die thierisch-elektrischen Versuche. *Annalen der Physik*, 1853. 165(6): p. 211–233.
5. Lee, W.Y., J.G. Kim, and C.N. Chu, Micro fabrication of aluminum oxide patterns using local anodization. *International Journal of Precision Engineering and Manufacturing*, 2015. 16(13): p. 2623–2630.
6. Jameson, E.C., *Electrical discharge machining*. 2001: Society of Manufacturing Engineers.
7. Ito, T. and N. Kubo, Method for forming perforations in metal sheets by etching. 1972, Google Patents.
8. Nara, M., et al. Phase controllability improvement for alternating phase shift mask. in 18th Annual BACUS Symposium on Photomask Technology and Management. 1998. International Society for Optics and Photonics.
9. Lim, H.-T. and Y.-K. Kim. Novel fabrication of comb actuator using RIE of polysilicon and (110) Si anisotropic bulk etching in KOH. in *Micromachining and Microfabrication*. 1998. International Society for Optics and Photonics.
10. Huang, R., K.R. Hebert, and L.S. Chumbley, Microscopic observations of voids in anodic oxide films on aluminum. *Journal of The Electrochemical Society*, 2004. 151(7): p. B379–B386.

11. Vrublevsky, I., et al., Study of chemical dissolution of the barrier oxide layer of porous alumina films formed in oxalic acid using a re-anodizing technique. *Applied Surface Science*, 2004. 236(1): p. 270–277.
12. Chung, C.K., et al., Hybrid pulse anodization for the fabrication of porous anodic alumina films from commercial purity (99%) aluminum at room temperature. *Nanotechnology*, 2009. 20(5): p. 055301.
13. Oh, H.J., K.W. Jang, and C.S. Chi, Impedance characteristics of oxide layers on aluminium. *Bulletin of the Korean Chemical Society*, 1999. 20(11): p. 1340–1344.
14. Park, J., et al., Fabrication of aluminum/alumina patterns using localized anodization of aluminum. *International Journal of Precision Engineering and Manufacturing*, 2012. 13(5): p. 765–770.
15. Jeon, S.I. and W.S. Chung, An Influence of Current density and Temperature about Anodic Oxidation Film Properties of Al Die-casting. 2014.
16. Kock, M., V. Kirchner, and R. Schuster, Electrochemical micromachining with ultrashort voltage pulses—a versatile method with lithographical precision. *Electrochimica Acta*, 2003. 48(20): p. 3213–3219.
17. Bhattacharyya, B. and J. Munda, Experimental investigation on the influence of electrochemical machining parameters on machining rate and accuracy in micromachining domain. *International Journal of Machine Tools and Manufacture*, 2003. 43(13): p. 1301–1310.
18. KM Kang, E.P., SS Kim, Effect of sulfuric-oxalic acid electrolyte on the formation of aluminum anodic oxide films. *Seoul National University of Technology, Research bulletin*, 1997. 46(1): p. 71–85.
19. Datta, M. and D. Landolt, Electrochemical machining under pulsed current conditions. *Electrochimica acta*, 1981. 26(7): p. 899–907.

20. Mahdavi, M., Z. Atlasbaf, and K. Forooraghi, A very compact CPW-FED ultra-wideband circular monopole antenna. *Microwave and Optical Technology Letters*, 2012. 54(7): p. 1665–1668.
21. Alvarez, A.L., C. Coya, and M. Garcia-Velez, Development of electrical-erosion instrument for direct write micro-patterning on large area conductive thin films. *Review of Scientific Instruments*, 2015. 86(8): p. 084704.
22. Lee, J., et al., Heat dissipation performance of metal-core printed circuit board prepared by anodic oxidation and electroless deposition. *Thermochimica acta*, 2014. 589: p. 278–283.
23. Takahashi, H., et al., Electron-microscopy of porous anodic oxide films on aluminum by ultra-thin sectioning technique, Part I. *Journal of Electron Microscopy*, 1973. 22(2): p. 149–157.
24. Paik, W.K.a.P. et al., *Electrochemistry: Science and Technology of electrode processes*. 2001, Seoul: Cheongmoongak.

## 국문 초록

본 연구에서는 양면 국부화 아노다이징 공정을 통해 알루미늄 호일에 절연성 산화 알루미늄 패턴을 생성하였다. 양면 국부화 아노다이징을 통해 기존 국부화 아노다이징 공정에 비해 생산성 향상과 세장비 향상이 가능했다. 본 연구에서 개발된 양면 국부화 아노다이징 공정을 통해 40  $\mu\text{m}$  두께의 알루미늄 호일을 관통하는 절연성 산화 알루미늄 패턴 생성이 가능했다. 원하는 패턴이 양각으로 새겨진 두 개의 동일 형상의 틀을 가공물 양쪽으로 접근시키고, 전해액에 담근 후 펄스 전압을 인가하면 해당 부분에 산화 알루미늄 층이 형성된다. 본 연구는 크게 세 가지 단계로 구성되어있다. 첫 번째는 양면 국부화 아노다이징 공정을 위한 가공 시스템 구축이다. 두 번째는 간극, 인가 전압, 펄스 조건 등의 실험 인자가 가공 결과에 미치는 영향을 관찰하고 최적 공정 조건을 선정하기 위한 실험을 진행하였다. 세 번째로 개발된 양면 국부화 아노다이징 기술을 활용하여 알루미늄 호일에 안테나 형상의 산화 알루미늄 패턴을 생성하여 단일면 RF 안테나를 제작하였다.

**키워드:** 국부화 아노다이징, 산화 알루미늄, 마이크로 전기 화학 공정,

**학번:** 2014-22503